Accepted Manuscript

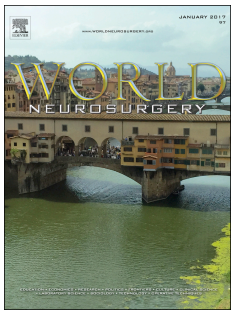

Quantifying Hemodynamics Changes in Moyamoya Disease Based on 2D Cine Phase-Contrast MRI and Computational Fluid Dynamics

Wenbo Sun, Zhao Ruan, Xuan Dai, Sirui Li, Shuo Li, Jianjian Zhang, Jincao Chen, Heye Zhang, Haibo Xu

PII: S1878-8750(18)32103-X

DOI: 10.1016/j.wneu.2018.09.057

Reference: WNEU 10262

To appear in: *World Neurosurgery*

Received Date: 5 June 2018

Revised Date: 6 September 2018

Accepted Date: 9 September 2018

Please cite this article as: Sun W, Ruan Z, Dai X, Li S, Li S, Zhang J, Chen J, Zhang H, Xu H, Quantifying Hemodynamics Changes in Moyamoya Disease Based on 2D Cine Phase-Contrast MRI and Computational Fluid Dynamics, *World Neurosurgery* (2018), doi: https://doi.org/10.1016/j.wneu.2018.09.057.

Quantifying Hemodynamics Changes in Moyamoya Disease Based on 2D Cine Phase-Contrast MRI and Computational Fluid Dynamics

Wenbo Sun[a, †], Zhao Ruan[a,†], Xuan Dai[b], Sirui Li[a], Shuo Li[c], Jianjian Zhang[b], Jincao Chen[b], Heye Zhang[d,*], Haibo Xu[a,*]

Affiliation:

[a] *Department of Radiology, Zhongnan Hospital of Wuhan University, Wuhan University, Wuhan, 430071, P. R. China*

[b] *Department of Neurosurgery, Zhongnan Hospital of Wuhan University, Wuhan University, Wuhan, 430071, P. R. China*

[c] *Department of Medical Biophysics, The University of Western Ontario, London, Ontario, N6A 4V2, Canada*

[d] *Shenzhen Institutes of Advanced Technology, Shenzhen, 518055, P. R. China*

† Wenbo Sun and Zhao Ruan contributed equally to the work.

* Correspondence: hy.zhang@siat.ac.cn, xuhaibo1120@hotmail.com

Corresponding Author:

All correspondence should be addressed to Dr. Haibo Xu.

E-mail: xuhaibo1120@hotmail.com

Tel: (+86) 027-67813057

Abbreviations:

CVR Cerebrovascular reserve
ICA Internal carotid artery
VA Vertebral artery
BA Basilar artery
PComA Posterior communicating artery
L_ Left
R_ Right
2D Two-dimensional
3D Three-dimensional
CFD Computational fluid dynamics
PC-MRI Phase-contrast MRI
HR TOF-MRA High resolution time of flight magnetic resonance angiography
WSS Wall shear stress
MMD Moyamoya disease
CoW Circle of Willis
PD Pressure drop
PDD Pressure drop difference
STA-MCA bypass Superficial temporal artery to middle cerebral artery bypass

Abstract

OBJECTIVE: This study aims to investigate hemodynamics changes in Moyamoya disease (MMD) by means of 2-dimensional cine phase contrast MRI (PC-MRI) and computational fluid dynamics (CFD).

MATERIALS AND METHODS: Eighteen MMD patients and ten healthy controls were enrolled. PC-MRI scans were conducted to quantify the flow rate of main supplying arteries including internal carotid arteries (ICAs) and vertebral arteries (VAs). Mean flow rate in these vessels was adopted as the patient-specific boundary condition for the CFD simulation of the Circle of Willis (CoW) in MMDs and controls. Pressure drop in both ICAs and their difference, wall shear stress and secondary flow in the carotid siphon of ICAs, and flow rate and size of posterior communicating arteries (PComAs) were compared between MMDs and controls. Four MMD patients underwent follow-up scans for longitudinal comparison.

RESULTS: PC-MRI data revealed significantly different flow rate in ICAs and VAs between MMDs and controls. CFD simulation demonstrated similar wall shear stress and similar secondary flow of both ICAs, but significantly higher pressure drop in the LICA, higher pressure drop difference (PDD) between LICA and RICA and higher flow rate in PComAs in MMDs as compared with controls. Significantly increased size of the LPComA in MMDs was also found. Furthermore, follow-up results confirmed that the combination of PDD, flow rate and size of PComAs has the potential to assist long-term prognosis after surgery.

CONCLUSIONS: PDD, flow rate and size of PComAs can be used to evaluate impairments in cerebrovascular reserve and indicate long-term prognosis in MMD.

Keywords:

Moyamoya disease, computational fluid dynamics, Circle of Willis, phase-contrast MRI, hemodynamics, cerebrovascular reserve

INTRODUCTION

Moyamoya disease (MMD) is a type of cerebrovascular disease characterized by the progressive stenosis of intracranial internal carotid arteries (ICAs), which is first described by Japanese neurosurgeons.[1] Reduced cerebral perfusion results in the progressive development of collateral vasculature in the form of small fragile vessels at the base of the brain.[2] The development of collateral vessels is accompanied with changes in cerebral hemodynamics. This process is always accompanied with serious symptoms, such as headache, transient ischemic attack (TIA) and ischemic stroke.[2] The majority of the suffering population is East Asian, involving both children and adults.[3]

Numerous advanced techniques have been attempted on early diagnosis and evaluation of MMD, including genetic analysis, EEG recordings and radiologic techniques. [3, 4] Based on Suzuki's grading system,[1] cerebral angiography imaging techniques are effective for diagnosing MMD and evaluating its progression. Xenon-enhanced CT, Positron emission tomography (PET), Single-photon-emission computed tomography (SPECT), perfusion CT and perfusion-weighted MRI have been widely used to quantify cerebral hemodynamics in MMD patients and could provide insights into regional hemodynamics, including cerebral blood flow (CBF), cerebral blood volume (CBV), time to peak (TTP) and mean transit time (MTT).[5-9] Because of the development of arterial spin labeling (ASL) MRI and blood oxygen level-dependent (BOLD) MRI, cerebral hemodynamics of MMD patients can be investigated non-invasively.[10, 11] However, above radiologic techniques could only measure hemodynamics in a specific region of interesting and suffer from poor spatial resolution. Other techniques could measure hemodynamics characteristics in specific vessels, such as pressure wire, transcranial doppler ultrasound (TCD) and

two-dimensional (2D) cine phase-contrast MRI (PC-MRI). [12, 13] Pressure wire is invasive and expensive. [13] TCD could measure the velocity and flow in a single 2D plane, but its performance is largely determined by the experience of the operator. 2D cine PC-MRI, as a non-invasive and accurate flow imaging method, has been applied to measure the flow rate and velocity in cerebral vasculature.[14] However, it is impractical to acquire the whole brain cerebral hemodynamics using PC-MRI due to the long scan time.

Recently, computational fluid dynamics (CFD) based on non-invasive imaging technique has emerged as one powerful tool to evaluate hemodynamics in cerebrovascular diseases. Compared with TCD and PC-MRI, CFD could demonstrate complex hemodynamic features with high spatial and temporal resolution (Sarrami-Foroushani et al., 2015).[15] Previous studies have already tested the CFD simulation to investigate the cerebral hemodynamics in MMD patients.[16-18] Cerebral hemodynamics changes in MMD patients treated by the Encephalo-duro-arterio-synangiosis surgery and the superficial temporal artery to middle cerebral artery (STA-MCA) bypass surgery have been studied with the CFD simulation.[16, 17] In pediatric MMD patients, CFD simulation was performed and hemodynamics features in ICAs were compared between children with MMD and healthy controls.[18] Both Karunanithi et al. and Zhu et al. used TCD to measure patient-specific boundary conditions,[16, 17] and Jamil et al. used boundary conditions calculated from empirical values.[18] Besides, Karunanithi et al. did not simulate collateral arteries in the simulation of the Circle of Willis (CoW), [16] while Zhu et al. and Jamil et al. only simulated ICA.[17, 18] Moreover, CFD combined with PC-MRI to investigate differences in the hemodynamics in the CoW between adult MMD patients and age-matched controls is yet to be reported.

This study was designed to quantify cerebral hemodynamic differences in the CoW between

MMD patients and age-matched controls, and hemodynamic changes after STA-MCA bypass surgery, using 2D cine PC-MRI and CFD. The result of this study might provide a more comprehensive understanding about MMD related hemodynamic changes, which can benefit the diagnosis and evaluation of MMD.

MATERIAL AND METHODS

Subjects

Eighteen patients (eleven males and seven females, mean age: 44.4 ± 9.1 years) diagnosed with MMD and ten healthy age-matched (six males and four females, age: 53.5±5.8 years) controls were recruited. Before the experiment, all subjects provided written informed consent, which was subject to approval by the ethics committee of the Zhongnan Hospital of Wuhan University. Among these MMD subjects, RICA was missing in two patients and LICA was missing in two other patients.

Imaging and data acquisition

Each subject underwent a high-resolution time of flight magnetic resonance angiography (HR TOF-MRA) scan using the Siemens Prisma 3T MRI (Siemens, Erlangen, Germany). The scanning parameters used in this study were: 6 slabs with -20% overlap, 40 slices per slab, repetition time (TR) = 21ms, echo time (TE) = 3.1ms, field of view (FOV) = 181 × 181 mm^2, flip angle = 20°, slice thickness = 0.5mm, matrix = 331×384, voxel=0.26×0.26×0.5mm^3. Three-dimensional (3D) patient-specific geometry of the CoW was then reconstructed by processing TOF-MRA images with the commercial medical imaging processing software Mimics 21.0 (Materialise, Leuven, Belgium). During the reconstruction, basilar artery (BA), ICAs, vertebral arteries (VAs), middle cerebral arteries (MCAs), anterior cerebral arteries (ACAs),

posterior cerebral arteries (PCAs), the first branches of MCAs, ACAs, PCAs, communicating arteries, and collateral vessels were preserved. After MRA, PC-MRI was performed for the BA, ICAs, and VAs. The scanning parameters were: TR = 18ms, TE = 3.11ms, FOV =151.6 × 151.6 mm^2, flip angle = 20°, slice thickness = 3mm, matrix = 155×256. The encoding velocity was set at 100cm/s.

To investigate cerebral hemodynamics changes after STA-MCA bypass surgery, PC-MRI and TOF-MRA data were collected in four patients (subject 1-4) before the surgery, one week after surgery, and three months after surgery. Subject 3 only participated in scans before and three months after surgery, due to a hemorrhagic infarction in the frontal lobe one week after surgery. Subject 4 only participated in scans before and one week after surgery. Acute intracranial hemorrhage was detected on subject 1 during the follow-up. According to the analysis of clinical grading scales, deterioration in surgical outcome was found in subject 1. There was no improvement and deterioration in surgical outcome in subject 2 and subject 3, and there was improvement in subject 4.

Computational modeling

The geometry of the CoW was exported as a STL format file from Mimics and imported into the CFD front-end software ANSYS ICEM CFD (14.0, ANSYS Inc., Canonsburg, PA, USA). The Quick (Delaunay) mesh procedure was employed in ICEM CFD and generated about 2 million mixed tetra/hybrid elements in an unstructured format for each case. A mesh convergence study was performed with coarser and finer meshes. The blood was assumed to be incompressible, laminar Newtonian fluid and follow the continuity equation (eq.1) and the momentum equation (eq.2):[19]

$$\nabla \cdot \mathrm{V} = 0 \quad (1)$$

$$\frac{\partial \mathrm{V}}{\partial \mathrm{t}} + (\mathrm{V} \cdot \nabla)\mathrm{V} = -\frac{1}{\rho}\nabla p + f + \frac{\mu}{\rho}(\nabla^2 V) \quad (2)$$

Where ρ is the density of blood and set to 1060 kg/m3, μ is the dynamic viscosity and set to be 0.0035 Pa·s, p is the pressure, V is the velocity field, and f is the body force and set to be zero. The vascular wall was assumed rigid with non-slippery boundary condition. The inlet boundary condition used mass-flow boundary condition, while the outlet boundary condition used pressure outlet with zero pressure.

Data and statistical analysis

Firstly, the flow rate of the BA，ICAs, and VAs was compared respectively between MMD patients and healthy controls. After that, the accuracy of the CFD model was assessed by comparing the simulated velocity in the BA with PC-MRI measurements, and two-tailed paired Student's t test was performed. Then, the pressure drop in both ICAs and the pressure drop difference (PDD) between LICA and RICA were investigated. Carotid siphon is an important structure in the ICA. Wall shear stress (WSS) and secondary flow in the outer wall in the carotid siphon of both ICAs were investigated.[18] Secondary flow refers to the flow superimposed over the primary axial flow, which could reflect in-plane velocity components.[18] The flow rate and size of posterior communicating arteries (PComAs) were also compared between MMD patients and controls in this study. Mean cross-sectional area of PComAs was used to quantify changes in the size of PComAs. All the statistical analysis was conducted in SPSS21.0 (SPSS Inc., Chicago, IL, USA). Independent samples Student's t test was performed for each variable between the MMD group and the control group. The significance level was set at $p<0.05$.

RESULTS

Figure 1 shows the mean flow rate in the BA, ICAs, and VAs of the MMD group and the healthy control group, respectively. The results indicated a significantly higher flow rate in the BA (P=0.030) and the RVA (P=0.038) in MMD patients than in controls. The results also showed significantly reduced flow rate in the LICA (P=0.009) in MMD patients than in controls.

Figure 2 compares PC-MRI measured results with simulation results in terms of the flow velocity in the BA in both MMD and control group, and there is no significant difference between the two. **Figure 3** demonstrates simulation results of the CoW in a MMD patient and a healthy control, including pressure distribution, wall shear stress and velocity amplitude. As shown in **Figure 4**, there were higher pressure drop in the RICA (P=0.061) and the LICA (P=0.014) on the MMDs when compared with the controls. Significantly higher PDD (P=0.007) between RICA and LICA was also found in the MMD group. The results showed similar WSS and similar secondary flow in the outer wall in the carotid siphon of both ICAs in MMD patients when compared with controls (**Figure 5**). Significantly increased flow rate in the RPComA (P=0.010) and the LPComA (P=0.010) (**Figure 6A**) and significantly increased cross-sectional area of the LPComA (P=0.013) were also observed in MMD patients (**Figure 6B**).

For the follow-up study, hemodynamic changes after STA-MCA bypass surgery in four patients (subjects 1-4) were demonstrated in **Figure 7**, including flow rate in the BA, ICAs, VAs and PComAs, pressure drop in ICAs, PDD between left and right ICA, and mean cross-sectional area of PComAs. For subject 1, the surgical side was right. As shown in **Figure 7**, there was no decrease in PDD after surgery. An increase in the pressure drop (22.026 Pa) of the LICA, an increase in the flow rate (0.117 ml/s) and a decrease in the mean cross-sectional area (0.101 cm^2)

of the LPComA were found after surgery (**Figure 7)**. During the follow-up, it was found an obvious increase in the PDD (105.277 Pa) accompanied with acute intracranial hemorrhage. For subject 2, the surgical side was right. Because the LICA was missing, PDD could not be used to evaluate hemodynamics changes after surgery for subject 2. There was a decrease in the pressure drop (11.255 Pa) in the RICA in subject 2. The comparable flow rate and size of PComAs after surgery and during the follow-up in subject 2 were also demonstrated in **Figure 7**, while there was no improvement in surgical outcome. For subject 3, the surgical side was left. There was no obvious decrease in the PDD, and there was an increase in the flow rate (0.246 ml/s) and a decrease in the mean cross-sectional area (0.014 cm^2) of the LPComA during the follow-up, while there was no significant improvement in subject 3, too. For subject 4, the surgical side was left. Since both PComAs were missing, the flow rate and size of PComAs could not be used to evaluate hemodynamics changes after surgery for subject 4. As showed in the **Figure7,** there was a decrease in the pressure drop of the RICA (51.244 Pa) and the LICA (6.230 Pa) and a decrease in the PDD (43.894 Pa) in subject 4 after surgery, while subject 4 had a good surgical outcome. **Figure 8** showed the pressure contribution in subjects 1-4 before and after surgery, and during the follow-up.

DISCUSSION

This study aimed to use 2D cine PC-MRI combined with CFD to investigate hemodynamic differences in the CoW between MMD patients and healthy controls. Meanwhile, hemodynamics changes after STA-MCA bypass surgery in four MMD patients were studied. Compared with PC-MRI measurements, simulation results showed similar flow velocity in the BA in both MMD and control group, which implied that the CFD model applied in this study could be used to

describe cerebral hemodynamic characteristics in the CoW in MMD patients. Simulation results demonstrated significantly higher pressure drop in the LICA, higher PDD between LICA and RICA, similar WSS and similar secondary flow in the outer wall in the carotid siphon of both ICAs, and higher flow rate in PComAs in the MMD group when compared with the control group. Besides, significantly increased size of the LPComA was found in MMD patients.

Compared with healthy controls, the significantly higher flow rate in the BA and VAs and the significantly lower flow rate in ICAs measured by PC-MRI in the MMD group were in agreement with a previous study.[14] Generally, patient-specific boundary conditions could be directly measured by pressure wire, TCD or 2D cine PC-MRI. 2D cine PC-MRI was most suggested thanks to its accuracy and non-invasiveness.[20] Besides, patient-specific boundary conditions could also be calculated from vascular resistances, but the calculation process needs an empirical value or the average flow data measured from healthy controls as a reference.[18, 21] However, previous studies suggested that the calculated patient-specific boundary condition might lead to a overestimation or underestimation of simulation results.[12, 22] Since the CFD simulation was sensitive to boundary conditions,[23] PC-MRI results indicated that it was necessary to use measured patient-specific boundary conditions for accurate simulation, due to the very different flow rate in ICAs and VAs between MMD patients and controls.

The considerably higher pressure drop found in the LICA in the MMD group compared with the healthy control group might be the results of the ICA stenosis. Previous study showed that with severe ICA stenosis, there was significantly increased pressure drop in the ICA.[24] Increased pressure drop has been suggested to be a predictor of poor surgical outcome after surgical treatment in MMD patients in previous studies. [16, 17] It was found that in MMD patients treated

253 with direct or indirect revascularization surgery, those improved patients had an observable
254 decrease in the pressure drop in the ICA after surgery, while the other patients had similar or
255 increased pressure drop.[16, 17] Follow-up results in subject 1, 3 and 4 in this study agreed with these
256 previous findings. [16, 17] As for the WSS and the secondary flow, previous study has found
257 increased WSS and decreased secondary flow in the outer wall in the carotid siphon of ICAs in
258 pediatric MMD patients as compared with healthy controls.[18] The non-significant difference in
259 WSS and secondary flow in the carotid siphon of both ICAs between MMD patients and healthy
260 controls found in this study were inconsistent with findings in pediatric MMD patients,[18] which
261 might be due to differences in pathological features between adult and pediatric patients, as well
262 as that ICAs in pediatric MMD patients are less developed.[25, 26] The similar WSS and similar
263 secondary flow found in this study might also be due to the complex changes in the vascular
264 geometry and the reduced blood flow in ICAs in MMD patients.[18] What's more, these findings
265 also indicated that WSS and secondary flow in the outer wall in the carotid siphon of both ICAs
266 might not be used in clinic as an index to help the evaluation and diagnosis in adult MMD same as
267 that in pediatric MMD.

268 The significantly higher PDD between RICA and LICA found in MMD patients indicated an
269 imbalance in the hemodynamics between the left and right side of the CoW. Previous study has
270 suggested that the brain could redistribute blood flow and keep the pressure distribution
271 symmetric to both sides of the CoW.[24] This imbalance in the pressure distribution in the CoW (as
272 showed in **Figure 3**) implies deficits in the cerebrovascular reserve (CVR) in MMD patients.
273 Besides, the significantly increased flow rate in both PComAs revealed by CFD simulation
274 indicated increased blood flow redistribution between the anterior circulation and the posterior

275 circulation. Previous study has already suggested that the dilatation of the PComA is a predictor of
276 intracranial bleeding in MMD patients.[27] In this study, the significantly increased size of the
277 LPComA in MMD patients compared with controls might imply an impaired vasodilatory reserve
278 and a decreased CVR. Besides, increased flow rate and decreased size of the LPComA were
279 simultaneously found after surgery in subject 1 and subject 3, which might be due to the
280 flow-induced vascular remodeling.[28] Therefore, PDD, flow rate and size of PComAs might be
281 utilized to evaluate CVR changes and predict the long-term prognosis after surgery in MMD
282 patients. Increased PDD after surgery may indicate an imbalance in the hemodynamics between
283 the left and right part of the CoW and be associated with a decrease in CVR. Increased flow rate
284 and decreased size in the LPComA after surgery may indicate an increased blood distribution
285 between the anterior and posterior circulation and an impaired CVR. Since some patients may
286 have missed the ICA or the PComA, it should be noted that the long-term prognosis after
287 STA-MCA bypass surgery might be well predicted by the combination of the PDD, the flow rate
288 and size of PComAs. More cases should be investigated to determine the relationship between
289 PDD, flow rate and size of PComAs with the CVR change and the long-term prognosis after
290 STA-MCA bypass surgery.

291 One limitation of this study is the fact that we used the steady flow analysis with rigid wall
292 assumption. The transient flow analysis could provide more comprehensive cerebral
293 hemodynamics information.[29] The use of Newtonian viscosity is also a limitation, which might
294 lead to the overestimation of the WSS.[30] Besides, to validate the accuracy of our CFD simulation,
295 only the flow velocity in the BA between PC-MRI measurements and simulation results were
296 compared in this study. It might be more convincing to compare all vessels, despite of a huge

297 amount of work. Moreover, although a previous study has used TOF-MRA scan to acquire the
298 geometry of the CoW,[16] there are too small collateral vessels to be captured. These small collateral
299 vessels might influence the accuracy of the CFD simulation. Computed tomograph angiography
300 (CTA) and 3D digital subtraction angiography (DSA) can also image collateral vessels in MMD
301 patients, but they are invasive due to the contrast agent injection. In this study, we used a HR
302 TOF-MRA scan and simulated collateral vessels in our CFD model, which has not been done in
303 previous studies.[16, 17]

304 **CONCLUSIONS**

305 In this work, CFD simulation combined with PC-MRI was used to non-invasively evaluate
306 cerebral hemodynamics in the CoW of MMD patients. PC-MRI results demonstrated that
307 patient-specific boundary condition was necessary for an accurate simulation in MMD patients.
308 CFD simulation demonstrated significantly higher pressure drop in the LICA, significantly higher
309 PDD between LICA and RICA, significantly increased flow rate in both PComAs and
310 significantly increased size of the LPComA in MMD patients as compared with healthy controls.
311 Moreover, follow-up studies in four MMD patients confirmed the potential of PDD together with
312 the flow rate and size of PComAs as indicators of the CVR change and the long-term prognosis
313 after STA-MCA bypass surgery. In the future, more long-term follow-up studies should be
314 performed to further examine these hemodynamic factors and their relationship with the CVR.

315

316 **Conflict of Interest Statement：**

317 The authors declare that they have no conflict of interest.

318

ACKNOWLEDGEMENTS

This work was supported by the National Natural Science foundation of China (Grant no. 81571734) .

REFERENCES

1. Suzuki J, Takaku A. Cerebrovascular “moyamoya” disease. Disease showing abnormal net-like vessels in base of brain. Arch Neurol.1969;20:288–299.

2. Scott RM, Smith ER. Moyamoya Disease and Moyamoya Syndrome. N Engl J Med. 2009;(12):1226-1237.

3. Hishikawa T, Sugiu K, Date I. Moyamoya Disease: A Review of Clinical Research. Acta Med Okayama. 2016;70(4):229-36.

4. Suzuki J, Kodama N. Moyamoya disease--a review. Stroke.1983;14(1):104-109.

5. Togao O, Mihara F, Yoshiura T, Tanaka A, Noguchi T, Kuwabara Y, Kaneko K, Matsushima T, Honda H. Cerebral hemodynamics in Moyamoya disease: correlation between perfusion-weighted MR imaging and cerebral angiography. AJNR Am J Neuroradiol. 2006;27(2):391-397.

6. Yang Y, Sun X, Han K. Study of the evaluation effect of Xe-CT to the CBF of patients with moyamoya disease. Journal of Apoplexy & Nervous Diseases. 2008;25(1):71-72.

7. Park SA, Yang CY, Choi SS, Kim WH. Assessment of cerebral hemodynamics to acetazolamide using brain perfusion SPECT in cerebral autosomal dominant arteriopathy with subcortical infarcts and leukoencephalopathy. Clin Nucl Med. 2011;36(2):158-159.

8. Kuhn FP, Warnock G, Schweingruber T, Sommerauer M, Buck A, Khan N. Quantitative H2[(15)O]-PET in Pediatric Moyamoya Disease: Evaluating Perfusion before and after Cerebral Revascularization. J Stroke Cerebrovasc Dis. 2015;24(5):965-971.

9. Chen Y, Xu W, Guo X, Shi Z, Sun Z, Gao L, Jin F, Wang J, Chen W, Yang Y. CT perfusion

342 assessment of Moyamoya syndrome before and after direct revascularization (superficial temporal
343 artery to middle cerebral artery bypass). European Radiology, 2016;26(1):254-261.
344 10. Thomas B, Logan W, Donner EJ, Shroff M. Assessment of cerebrovascular reactivity using
345 real-time BOLD fMRI in children with moyamoya disease: a pilot study. Childs Nerv Syst.
346 2013;29(3):457-463.
347 11. Noguchi T, Kawashima M, Nishihara M, Egashira Y, Azama S, Irie H. Noninvasive method for
348 mapping CVR in moyamoya disease using ASL-MRI. Eur J Radiol. 2015;84(6):1137-1143.
349 12. Liu X, Gao Z, Xiong H, Ghista D, Ren L, Zhang HY, Wu W, Huang W, Hau WK.
350 Three-dimensional hemodynamics analysis of the circle of Willis in the patient-specific
351 nonintegral arterial structures. Biomech Model Mechanobiol. 2016;15(6):1439-1456.
352 13. Liu J, Yan Z, Pu Y, Shiu WS, Wu J, Chen R, Leng X, Qin H, Liu X, Jia B, Song L, Wang Y,
353 Miao Z, Wang Y, Liu L, Cai XC. Functional assessment of cerebral artery stenosis: A pilot study
354 based on computational fluid dynamics. J Cereb Blood Flow Metab. 2017;37(7):2567-2576.
355 14. Neff KW, Horn P, Schmiedek P, Düber C, Dinter DJ. 2D cine phase-contrast MRI for volume
356 flow evaluation of the brain-supplying circulation in moyamoya disease. AJR Am J Roentgenol.
357 2006;187(1):107-115.
358 15. Sarrami-Foroushani A, Nasr Esfahany M, Nasiraei Moghaddam A, Saligheh Rad H, Firouznia
359 K, Shakiba M, Ghanaati H, Wilkinson ID, Frangi AF.. Velocity Measurement in Carotid Artery:
360 Quantitative Comparison of Time-Resolved 3D Phase-Contrast MRI and Image-based
361 Computational Fluid Dynamics. Iran J Radiol. 2015;12(4):e18286.
362 16. Karunanithi K, Han C, Lee CJ, Shi W, Duan L, Qian Y. Identification of a hemodynamic
363 parameter for assessing treatment outcome of EDAS in Moyamoya disease. J Biomech.

2015;48(2):304-309.

17. Zhu F, Karunanithi K, Qian Y, Mao Y, Xu B, Gu Y, Zhu W, Chen L, Wang Y, Pan H, Liao Y, Morgan M. Assessing surgical treatment outcome following superficial temporal artery to middle cerebral artery bypass based on computational haemodynamic analysis. J Biomech. 2015 26;48(15):4053-4058.

18. Jamil M, Tan GX, Huq M, Kang H, Lee ZR, Tang PH, Hu XH, Yap CH. Changes to the geometry and fluid mechanics of the carotid siphon in the pediatric Moyamoya disease.. Comput Methods Biomech Biomed Engin. 2016;19(16):1760-1771.

19. Bathe KJ. *Finite Element Procedures In Engineering Analysis*. Prentice-Hall, Inc, 1982.

20. Oktar SO, Yücel C, Karaosmanoglu D, Akkan K, Ozdemir H, Tokgoz N, Tali T. Blood-flow volume quantification in internal carotid and vertebral arteries: comparison of 3 different ultrasound techniques with phase-contrast MR imaging. AJNR Am J Neuroradiol. 2006;27(2):363-369.

21. Moore S, David T, Chase JG, Arnold J, Fink J. 3D models of blood flow in the cerebral vasculature. J Biomech. 2006;39(8):1454-1463.

22. McGah PM, Levitt MR, Barbour MC, Morton RP, Nerva JD, Mourad PD, Ghodke BV, Hallam DK, Sekhar LN, Kim LJ, Aliseda A. Accuracy of computational cerebral aneurysm hemodynamics using patient-specific endovascular measurements. Ann Biomed Eng. 2014;42(3):503-514.23.

23. Hoi Y, Wasserman BA, Lakatta EG, Steinman DA. Carotid bifurcation hemodynamics in older adults: effect of measured versus assumed flow waveform. J Biomech Eng. 2010;132(7):071006.

24. Long Q, Luppi L, König CS, Rinaldo V, Das SK. Study of the collateral capacity of the circle of Willis of patients with severe carotid artery stenosis by 3D computational modeling. J Biomech.

2008;41(12):2735-2742.

25. Hishikawa T, Tokunaga K, Sugiu K, Date I. Assessment of the difference in posterior circulation involvement between pediatric and adult patients with moyamoya disease. J Neurosurg. 2013;119(4):961-965.

26. Takagi Y, Hermanto Y, Takahashi JC, Funaki T, Kikuchi T, Mineharu Y, Yoshida K, Miyamoto S. Histopathological Characteristics of Distal Middle Cerebral Artery in Adult and Pediatric Patients with Moyamoya Disease. Neurol Med Chir (Tokyo). 2016;56(6):345-349.

27. Morioka M, Hamada J, Kawano T, Todaka T, Yano S, Kai Y, Ushio Y. Angiographic dilatation and branch extension of the anterior choroidal and posterior communicating arteries are predictors of hemorrhage in adult moyamoya patients. Stroke. 2003; 34(1):90-95.

28. Gibbons GH, Dzau VJ. The emerging concept of vascular remodeling. N Engl J Med. 1994;330(20):1431-1438.

29. Takeuchi S, Karino T. Flow patterns and distributions of fluid velocity and wall shear stress in the human internal carotid and middle cerebral arteries. World Neurosurg. 2010;73(3):174-185;

30. Xiang J, Tremmel M, Kolega J, Levy EI, Natarajan SK, Meng H. Newtonian viscosity model could overestimate wall shear stress in intracranial aneurysm domes and underestimate rupture risk. J Neurointerv Surg. 2012;4(5):351-357.

Figure Captions:

Figure 1. The comparison of the mean flow rate (mean ± standard error, SE) in main supplying arteries in the Circle of Willis (CoW) between the MMD group and the healthy control group. (BA: basilar artery, RICA: right internal carotid artery, LICA: left internal carotid artery, RVA: right vertebral artery, LVA: left vertebral artery.) (*: $P \leq 0.05$)

Figure 2. The mean flow velocity (mean ± standard error, SE) in the basilar artery (BA) acquired by CFD simulation and PC-MRI in the MMD group and the healthy control group.

Figure 3. An example of simulation results of a healthy control (A-C) and a MMD patient (D-F). An imbalance in the pressure distribution between the right internal carotid artery (RICA) and left internal carotid artery (LICA) in the MMD patient was showed in (D). ((A)(D): the contour of pressure; (B)(E): the contour of wall shear stress; (C)(F): velocity volume.)

Figure 4. The mean pressure drop (mean ± standard error, SE) in the right internal carotid artery (RICA) and the left internal carotid artery (LICA), and the mean pressure drop difference (PDD) between RICA and LICA in the MMD group and the healthy control group. (*: $P \leq 0.05$)

Figure 5. The mean wall shear stress (mean ± standard error, SE) (A) and the mean secondary flow (mean ± standard error, SE) (B) in the outer wall in the carotid siphon of the right internal carotid artery (RICA) and left internal carotid artery (LICA) in the MMD group and the healthy control group. (*: $P \leq 0.05$)

Figure 6. The mean flow rate (mean ± standard error, SE) (A) and the mean cross-sectional area (mean ± standard error, SE) (B) in the right posterior communicating artery (RPComA) and the left posterior communicating artery (LPComA) in the MMD group and the healthy control group. (*: $P \leq 0.05$)

Figure 7. The hemodynamic changes, including mean flow rate in the right internal carotid artery

(RICA) and left internal carotid artery (LICA), right vertebral artery (RVA) and left vertebral artery (LVA), basilar artery (BA), mean pressure drop in ICAs, mean PDD between RICA and LICA, and mean flow rate and mean cross-sectional area of posterior communicating arteries (PComAs) before and one week after the superficial temporal artery to middle cerebral artery (STA-MCA) bypass surgery, and during the follow-up were demonstrated. LICA was missing in subject2. Subject 3 participated in scans only before surgery and during the follow-up. Subject 4 participated in scans only before and after surgery. Besides, both PComAs were missing in subject 4. (S1: subject 1, S2: subject 2, S3: subject 3, S4: subject 4, PD: pressure drop, PDD: pressure drop difference between RICA and LICA, Pre: before the STA-MCA bypass surgery, Post: one week after the STA-MCA bypass surgery, Follow: three months after the STA-MCA bypass surgery.) (*: $P \leq 0.05$)

Figure 8. The pressure contribution in the CoW of subject 1-4 before and after surgery, and during the follow-up. (A)(D)(G)(J): before the STA-MCA bypass surgery; (B)(E)(K): one week after the STA-MCA bypass surgery; (C)(F)(H): three months after the STA-MCA bypass surgery. Subject 3 participated in scans only before surgery and during the follow-up. Subject 4 participated in scans only before and one week after surgery.

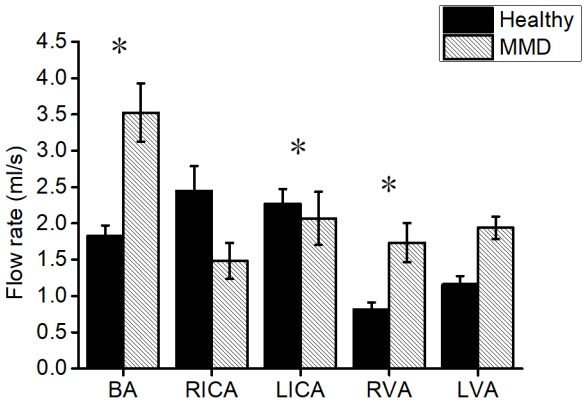

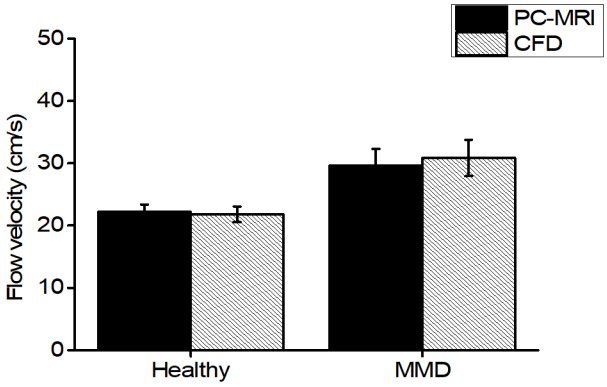

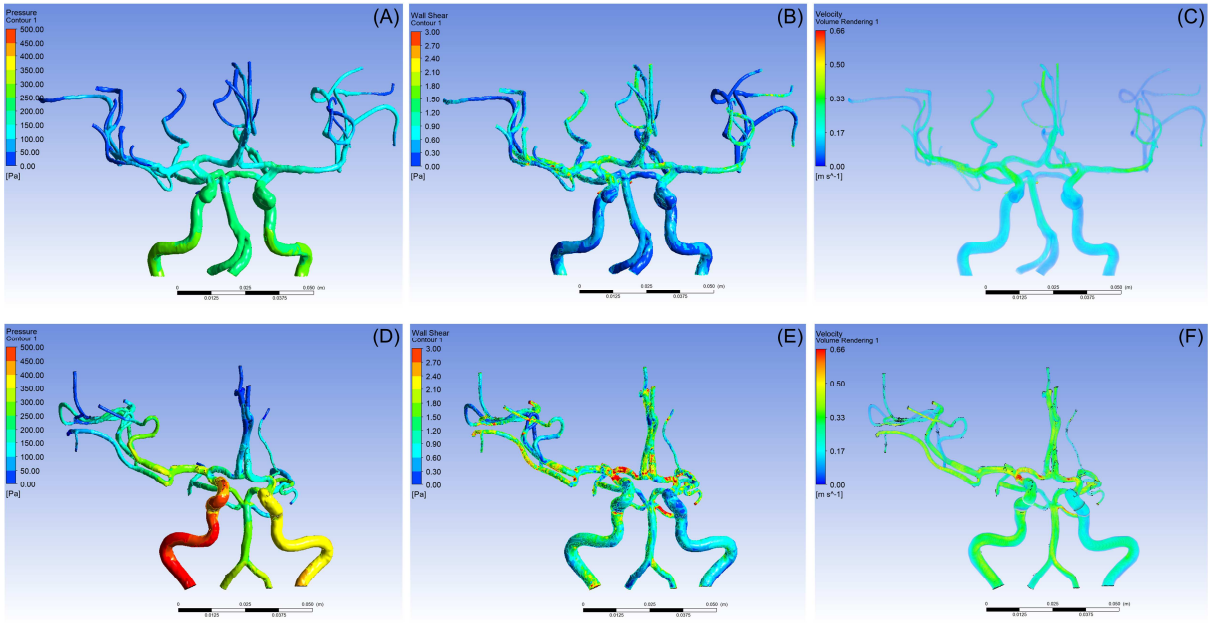

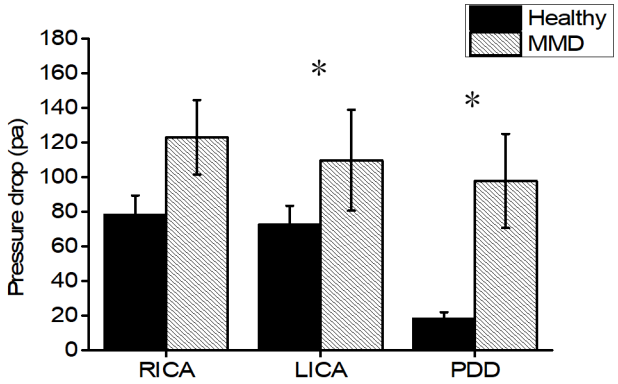

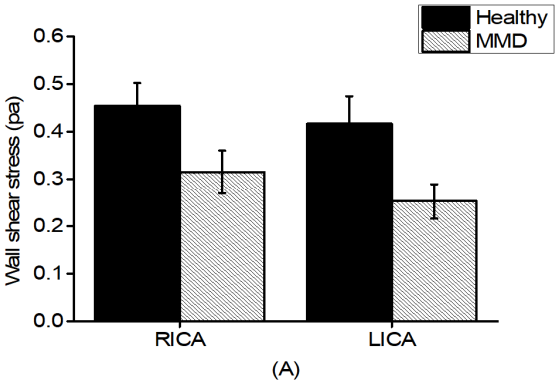

(A)

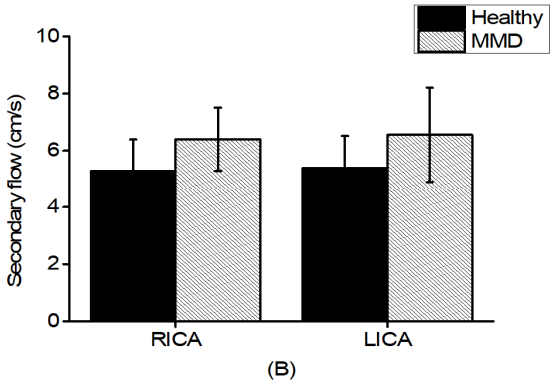

(B)

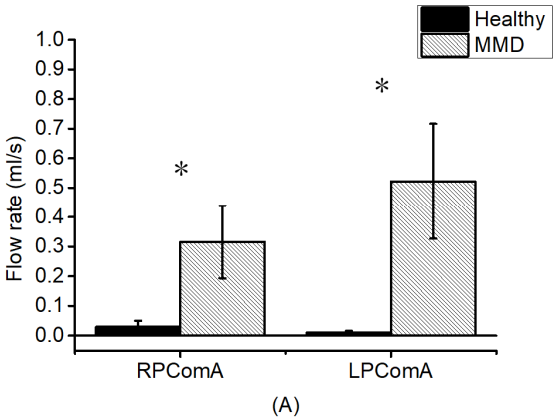

(A)

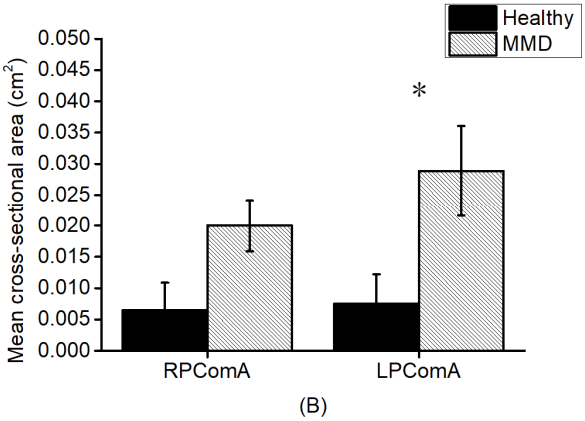

(B)

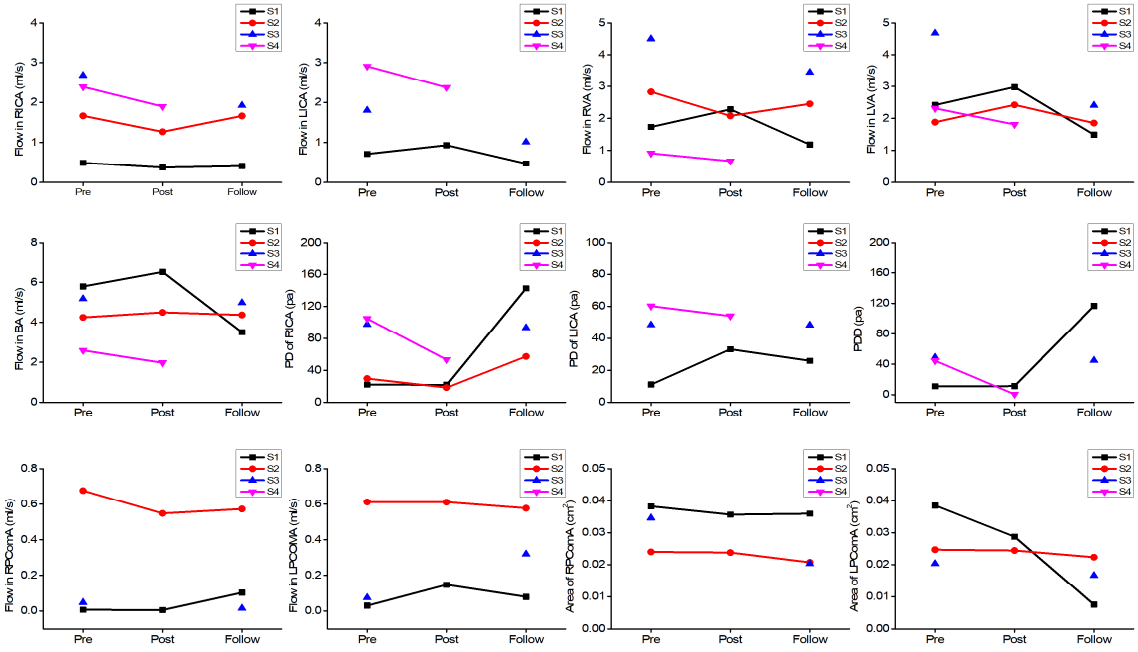

Subject 1

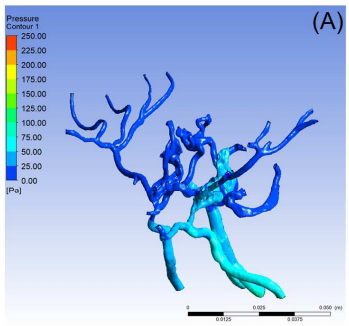

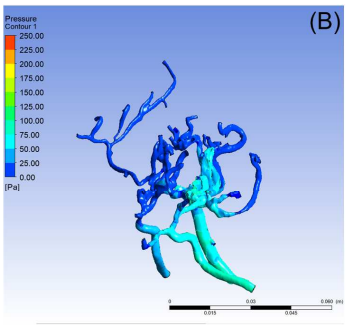

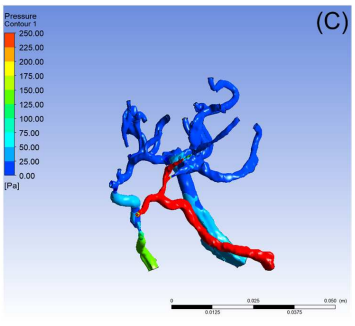

Subject 2

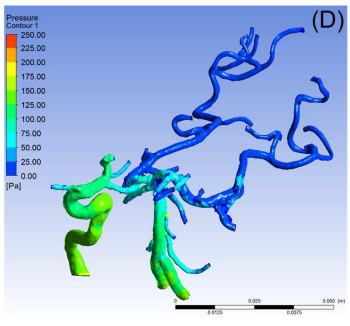

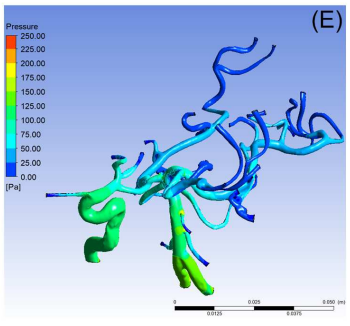

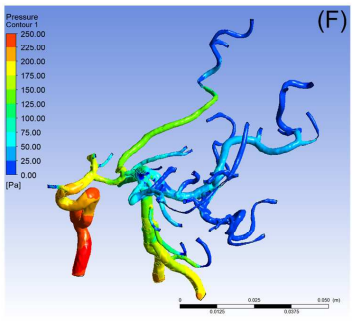

Subject 3

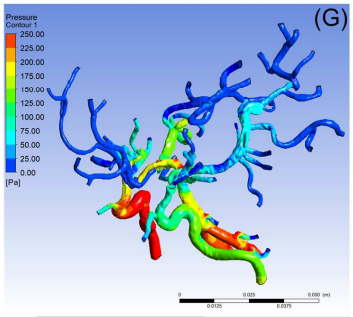

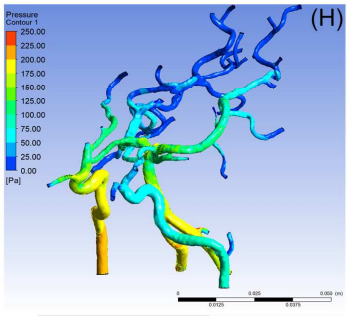

Subject 4

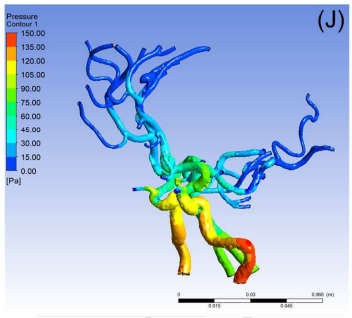

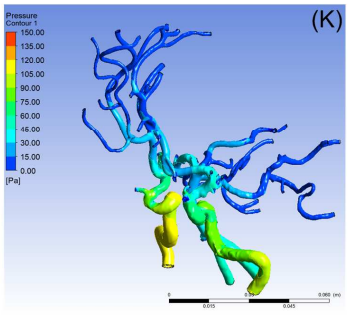

Highlights:

- Phase-contrast MRI and computational fluid dynamics can help evaluate CVR in MMD
- Wall shear stress and secondary flow in ICAs might not help evaluate CVR in adult MMD
- PDD between left and right ICA can evaluate CVR impairments in MMD
- Flow rate and size of PComAs can evaluate CVR impairments in MMD
- PDD together with flow rate and size of PComAs can predict surgical prognosis